Bioconvection-Driven Tangent Hyperbolic Nanofluid Flow with Chemical Reaction on Riga Plate

Moon Das., S.N. Mohapatra

Department of Mathematics, Bhattadev University, Assam, 781325, India

DOI: https://dx.doi.org/10.51584/IJRIAS.2026.110200133

Received: 01 March 2026; Accepted: 06 March 2026; Published: 19 March 2026

ABSTRACT

The ongoing research centres on the flow of tangent hyperbolic nanofluid over a Riga surface, affected by heat dissipation and radiative thermal effects. In the present study, the influence of nanofluid arises from the joint effects of Brownian motion and thermophoresis, driven by cross-diffusion phenomena and thermal radiation. As a novel approach, the bioconvection-induced motile microorganism, combined with higher-order chemical reactions, enriches the flow characteristics. The mathematical model obtained with the aforesaid assumptions is formulated and transmuted into dimensionless form by utilizing standard transformation rules. Moreover, the formulated problem is addressed numerically by utilizing the fourth-order Runge-Kutta approach via MATLAB's embedded bvp4c solver. The distinctive response of diverse variables governing the flow dynamics is depicted through graphical representations, subsequent to corroborating the findings with prior studies.

Keywords: Tangent hyperbolic nanofluid; Riga plate; Brownian and thermophoresis; motile microorganism; Numerical treatment.

INTRODUCTION

In recent years, manufacturing technologies for non-Newtonian fluids have often been preferred over Newtonian fluids due to their superior behaviour in complex processes. The addition of certain additives can enhance the performance of these fluids and also broaden their industrial relevance. Magnetohydrodynamics (MHD) is one of the important mechanisms for controlling the cooling rate and influencing desired outcomes. Within magnetohydrodynamic power generation, electricity is derived from the interplay between magnetic fields and electrically conductive fluids such as plasma or high-temperature gases. These systems are effective in producing a large amount of power with minimal impact to the environment. The impact of MHD on stretching materials of various geometries has been examined by [1–4]. Within chemical engineering, the tangent hyperbolic fluid framework provides an advantageous replacement for the classical Newtonian approach, offering superior efficiency, reliability, and practical utility. In the non-Newtonian model, tangent hyperbolic fluid stands out for its ability to capture fluid behaviour more accurately [5]. Malik et al. [6] employed the Keller-box method to analyse electrically conducting tangent hyperbolic fluid transportation influenced by an elastic cylinder. Recently, Amjad et al. [7] examined the flow of such fluids under magnetic fields and nanoparticle effects over a stretched sheet.

The concept of nanofluids, which are base fluids combined with nanoparticles, was first introduced by Choi [8]. Nowadays, nanofluids are widely used in modern engineering and industrial systems to improve thermal performance and energy efficiency. In particular, adding nanoparticles to base fluids significantly enhances thermal conductivity, thus improving heat transfer efficiency. Researchers have devoted considerable interest to their growing prominence over the past two decades. Heat transfer theory has become a major research area due to its vast applications in technology, agriculture, and moisture management. Cattaneo-Christov heat flux, combined with Ohmic heating and thermal absorption between Riga plates, was analysed in [9]. Rasool et al. [10] further explored electrically conducting fluid flows between Riga plates with thermal and nanoparticle effects.

ISSN No. 2454-6194 | DOI: 10.51584/IJRIAS |Volume XI Issue II February 2026

Bio-convection refers to the self-organized motion of motile microorganisms, which may involve single or clustered microbes. It often results from the tendency of certain microorganisms, like gyrotactic cells, to swim against gravity. In still fluids, these organisms exhibit directed motion, leading to bio-convective patterns. Vincent et al. [11] illustrated such bioconvection in algae suspensions. Kada et al. [12] assessed the consequences of gyrotactic microorganisms in a Williamson fluid influenced by radiative heat transfer, while Raizah et al. [13] studied gyrotactic microorganism behaviour in hybrid nanofluid flow near a stagnation point on a circular cylinder. The recent literature [14–28] shows a growing interest in bio-convection, but till today, very less comprehensive studies have examined the combined effects of swimming microorganisms in magnetized flow of tangent hyperbolic nanofluid with Joule heating. This work aims to incorporate the influence of a Riga plate to drive the flow. The influence of motile microorganisms is regarded as a crucial component of this study. The governing framework of coupled PDEs for tangent hyperbolic nanofluid flow is converted into an equivalent system of ODEs. Numerical simulations are carried out using the bv4c function in MATLAB to validate the results, and comparisons are made with earlier published works, showing strong consistency and reliability.

Objective of the current investigation: Based on the earlier investigations, the proposed study aims to present the following;

- The introduction of tangent hyperbolic, a non-Newtonian nanofluid with the interaction cross-diffusion effect over a Riga plate, is useful in various applications.
- The impact of Brownian and thermophoresis combined with dissipative heat, such as magnetic and Darcy dissipation, encourages the heat transport profiles.
- The bioconvection-induced motile microorganism with higher-order chemical reaction with different species characterizes the solutal distribution.
- The combined effect is utilized in the polymer extrusion processes and is also effective in drug delivery systems in hyperthermia treatment.

Mathematical Formulation:

An investigation has been carried out on the 2d stable magnetised fluid motion and thermal energy transfer. of a tangent hyperbolic nanofluid subjected to solar radiation and ohmic heating on a Riga plate (Fig.1), under the following assumptions:

- The surface is subjected to a steady magnetic field of magnitude B_0 oriented perpendicularly.
- The fluid momentum is represented as $V = V(u, v)$.
- The flow is generated by an expanding surface located along the plane $y = 0$.

The essential governing equations associated with this model are:

$$\frac{\partial u}{\partial x}+\frac{\partial v}{\partial y}=0 \tag{1}$$

$$u\frac{\partial u}{\partial x}+v\frac{\partial u}{\partial y}=\nu(1-n)\frac{\partial^2 u}{\partial y^2}+\sqrt{2}\nu n\Gamma\left(\frac{\partial u}{\partial y}\right)\frac{\partial^2 u}{\partial y^2}+\frac{\pi J_0 M_0}{8\rho_f}\exp\left(\frac{-\pi}{b}y\right)-\frac{\sigma B_0^2 u}{\rho_f}-\frac{\mu}{\rho K_p^*}u \tag{2}$$

$$u\frac{\partial T}{\partial x}+v\frac{\partial T}{\partial y}=\alpha\left(\frac{\partial^2 T}{\partial y^2}\right)+\tau\left[D_B\left(\frac{\partial C}{\partial y}\right)\left(\frac{\partial T}{\partial y}\right)+\frac{D_T}{T_\infty}\left(\frac{\partial T}{\partial y}\right)^2\right]+\frac{\sigma B_0^2 u^2}{(\rho C_p)_f}-\frac{1}{(\rho C_p)_f}\frac{\partial q_r}{\partial y} \tag{3}$$

$$u\frac{\partial C}{\partial x}+v\frac{\partial C}{\partial y}=D_B\frac{\partial^2 C}{\partial y^2}+\frac{D_T}{T_\infty}\left(\frac{\partial^2 T}{\partial y^2}\right)-K_1(C-C_\infty)^m \tag{4}$$

$$u\frac{\partial n}{\partial x}+v\frac{\partial n}{\partial y}+\frac{bWc}{(C_w-C_\infty)}\left[\frac{\partial}{\partial y}\left(n\frac{\partial C}{\partial y}\right)\right]=D_m\frac{\partial^2 n}{\partial y^2} \tag{5}$$

Along with the imposed boundary constraints

$$\left.\begin{aligned} &u=u_w, v=0, -K\frac{\partial T}{\partial y}=h_f(T_w-T), D_B\frac{\partial C}{\partial y}+\frac{D_T}{T_w}\frac{\partial T}{\partial y}=0, n=n_w \quad \text{at} \quad y=0\\ &U\to U_\infty, T\to T_\infty, C\to C_\infty, n\to n_\infty \ \text{as} \ y\to\infty \end{aligned}\right\} \tag{6}$$

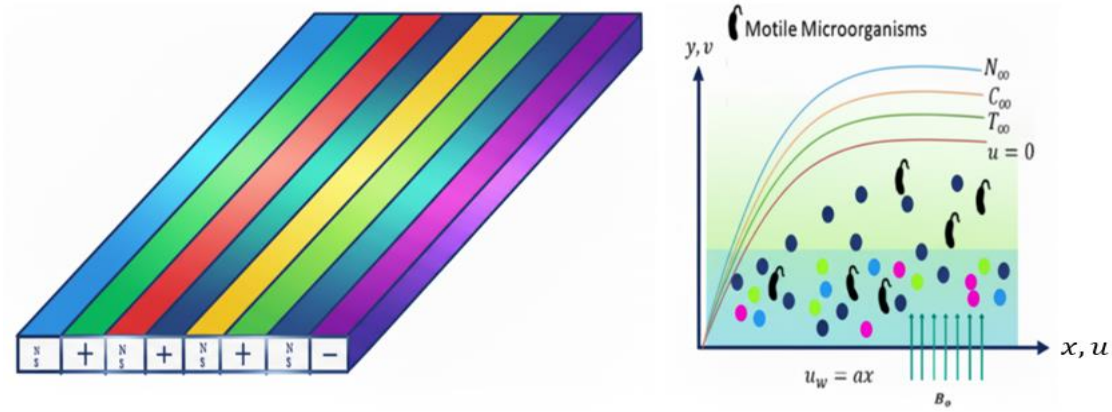

Fig.1 Physical model of the stretching Riga plate with motile microorganisms and an applied magnetic field.

Introducing the similarity transformation

$$\left.\begin{aligned} &\psi=\sqrt{a\nu}\,xf(\eta), \varphi(\eta)=\frac{C-C_\infty}{C_w-C_\infty}, \theta(\eta)=\frac{T-T_\infty}{T_w-T_\infty}, \chi(\eta)=\frac{n-n_\infty}{n_w-n_\infty}, \eta=\sqrt{\frac{a}{\nu}}y,\\ &u=\frac{\partial\psi}{\partial y}, v=-\frac{\partial\psi}{\partial x} \end{aligned}\right\} \tag{7}$$

As a result, equation (1) satisfies automatically and equations (2) to (5) are renovated as:

$$(1-n)f'''+ff''+nWe\,f''f'''-f'^2-Mf'-Da\,f'+Q\exp(-c_1\eta)=0 \tag{8}$$

$$\left(1+\frac{4}{3}R_d\right)\theta''+\Pr f\theta'+\Pr M\,E_c f'^2+\Pr Nb\,\theta'\varphi'+\Pr Nt\,\theta'^2+\Pr Ec\,Da\,f'^2=0 \tag{9}$$

$$\varphi''+\frac{Nt}{Nb}\theta''+Le\Pr f\varphi'-Le\Pr k_1C_\infty^{m-1}\varphi^m=0 \tag{10}$$

$$\chi''+Lb\,f\chi'-Pe\left[\varphi''(\chi+\Omega)+\chi'\varphi'\right]=0 \tag{11}$$

The boundary conditions are transformed as:

$$\left.\begin{aligned} &f(0)=0,\ f'(0)=1, \theta'(0)=Bi(\theta(0)-1), Nb\,\varphi'(0)+Nt\,\theta'(0)=0, \chi(0)=1 \ \text{at} \ \eta=0\\ &f'(\eta)\to 0, \theta(\eta)\to 0, \varphi(\eta)\to 0, \chi(\eta)\to 0 \ \text{as} \ \eta\to\infty \end{aligned}\right\} \tag{12}$$

ISSN No. 2454-6194 | DOI: 10.51584/IJRIAS |Volume XI Issue II February 2026

Here are the dimensionless parameters involved in the flow process, given as

$$\left.\begin{aligned} &We=\frac{\sqrt{2}a^{3/2}x\Gamma}{\sqrt{\nu}},\ M=\frac{\sigma B_0^2}{\rho_f a},\ Da=\frac{\nu}{aK_p^*},\ Q=\frac{\pi J_0 M_0}{8\rho_f a^2 x},C_1=\frac{\pi}{b}\sqrt{\frac{\nu}{a}}\\ &k_r=\frac{k_1}{a},\ Le=\frac{\alpha}{D_B},\ \Pr=\frac{\nu}{\alpha},\ Nt=\frac{(\rho c)_p D_T(T_w-T_\infty)}{(\rho c)_f \nu T_\infty},\ Nb=\frac{(\rho c)_p D_B C_\infty}{(\rho c)_f \nu}\\ &Lb=\frac{\nu}{D_m},\ Pe=\frac{bW_c}{D_m}\left(\frac{C_\infty}{C_w-C_\infty}\right),\ \Omega=\frac{n_\infty}{n_w-n_\infty},\ Ec=\frac{a^2x^2}{c_p(T_w-T_\infty)}\\ &R_d=\frac{4\sigma^* T_\infty^3}{\alpha(\rho c_p)_f k^*},\ Bi=\frac{h_f}{k}\sqrt{\frac{\nu}{a}} \end{aligned}\right\} \quad (13)$$

Physical quantities are of defined as:

$$\left.\begin{aligned} &C_f=\frac{\tau_w}{\rho u_w^2},\ Nu_x=\frac{xq_w}{k(T\to T_\infty)},\\ &\tau_w=\mu\left((1-n)\frac{\partial u}{\partial y}+\frac{u\Gamma}{\sqrt{2}}\left(\frac{\partial u}{\partial x}\right)^2\right)\\ &q_w=-k\left(1+\frac{16\sigma^* T_\infty^3}{3k^* k}\right)\frac{\partial T}{\partial y} \end{aligned}\right\} \quad (14)$$

The physical variables in dimensionless form are expressed as follows.

$$\left.\begin{aligned} &C_f\sqrt{Re}_x=-\left((1-n)+\frac{n}{2}W_c f''(0)\right)f''(0)\\ &Nu_x R\mathrm{e}_x^{-1/2}=-\left(1+\frac{4}{3}N_r\right)\theta'(0)\\ &Sh_x R\mathrm{e}_x^{-1/2}=-\varphi'(0)\\ &Nn_x R\mathrm{e}_x^{-1/2}=-\chi'(0) \end{aligned}\right\} \quad (15)$$

Where $R\mathrm{e}_x=\frac{ax^2}{\nu}$ is the local Reynolds number.

Table-1: Comparative evaluation of $f''(0)$ for various values of M when $n=We=Da=0$

M	Jawad et al. [29]	Present study
0	-1	-1
0.5	−1.11803	−1.11293
1	−1.41419	−1.41309

Validation with discussion

In this work, the non-Newtonian flow performance of a tangent hyperbolic nanofluid interacting with a Riga plate is investigated. The interplay of thermal and solutal cross-diffusion, along with Brownian and

thermophoretic mechanisms, defines the imposition of the nanofluid on the flow characteristics. Further, the dissipative heat, along with thermal radiation and higher-order chemical reaction, favours enhancing the flow behaviour. More specifically, the motile microorganism shows the impact of bioconvection as well as the coupling effect of the profiles significant for the heat and solutal transport properties. The modelled problem is renovated into dimensionless form by utilizing similarity rules, and further, a standard numerical technique is utilized through the implementation of MATLAB's bvp4c function. The characterizing behaviour of specific elements influencing the flow characteristics is deployed via graphs and then elaborated. The numerical simulation of skin friction in a particular case is presented in Table-1, validating the result with the study of Jawad et al. [29]. Further, the following section elaborates on the significant behaviour of other factors through graphs where the numerical range of the parameters is reported clearly.

Behaviour of M and Da:

In the non-Newtonian model, the applied magnetization affects the flow profiles, demonstrating the integration of the magnetic parameter (M), whereas transport via a permeable medium underscores the interpretation of porosity (Da). Fig.2 and Fig.3 showcase the behaviour of M and Da on the fluid momentum and the energy pattern. For the present analysis, the magnetic parameter M is examined over the range $0 \le M \le 3$.and projected in two distinct cases, such as $Da = 0$ where the transport via a clear fluid medium and $Da = 0.5$ where the transport occurs through a porous medium. In particular $M = 0$ signifies the flow behaviour without the impact of magnetization and $M = 0$ portrays the characteristic of magnetization that affects the flow phenomena. The alignment of magnetization normal to the flow direction generates a resistive force manifested as the Lorentz force. This has a standard tendency to resist the fluid momentum and therefore, the fluid momentum retards throughout. This behaviour leads to reduce the thickness of the velocity bounding surface, and the pattern is asymptotic to meet the requisite ambient condition far away from the plate. A prominent feature of the flow profile is revealed through variations in the medium's permeability. Owing to the elevated hindrance presented by the porous medium, the flow experiences a pronounced deceleration compared to motion through a clear fluid. Again, this deceleration gives rise to accumulated energy at the bottom surface of the plate. This accumulated energy moves up and boosts the heat transport mechanism. Consequently, growing the magnetism intensifies its influence on the thermal pattern of the fluid. Moreover, the increasing porosity, the stored energy also favours augmenting the profile.

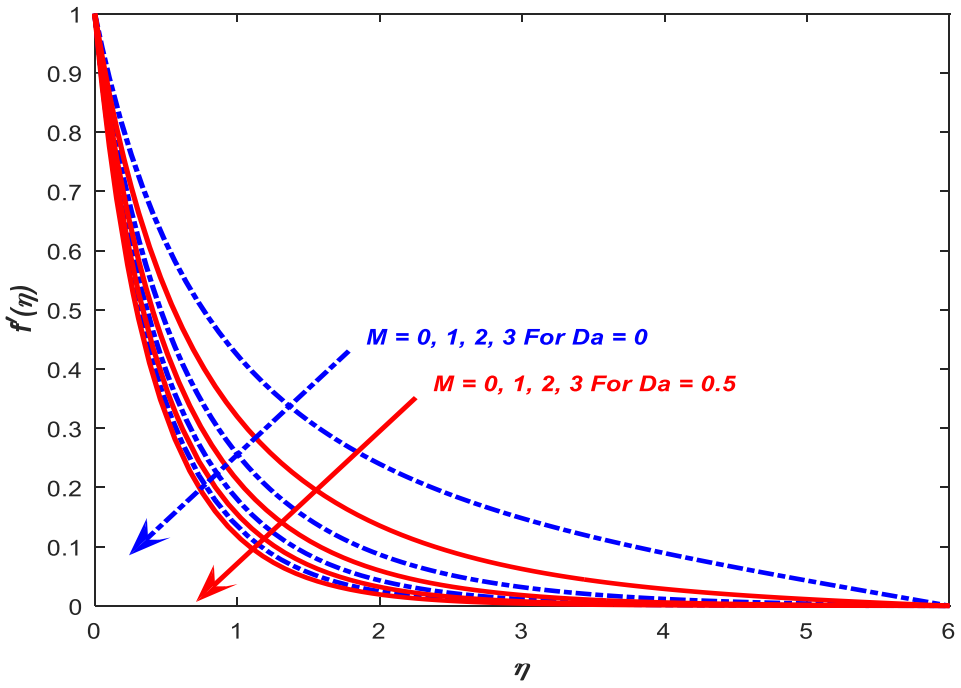

Fig.2 Various values of M on $f'(\eta)$

ISSN No. 2454-6194 | DOI: 10.51584/IJRIAS |Volume XI Issue II February 2026

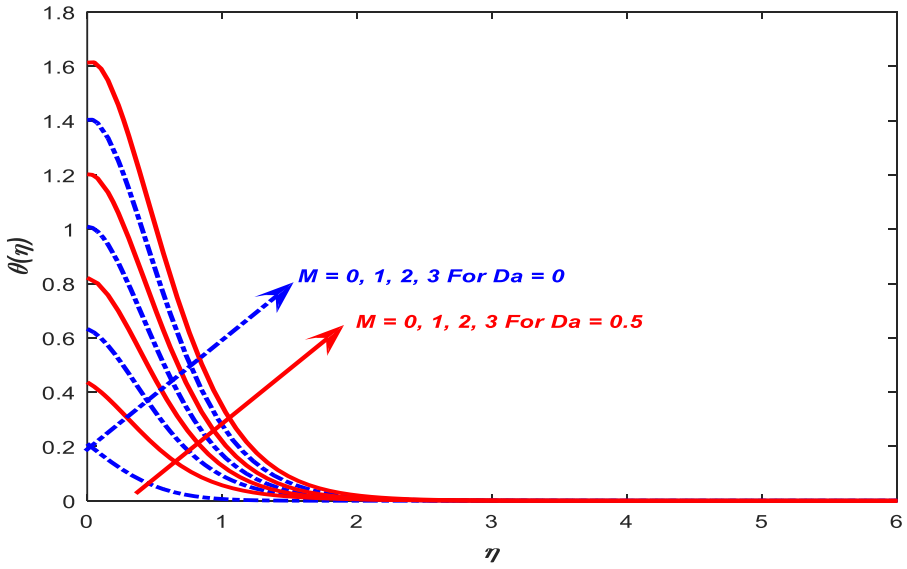

Fig.3 Various values of M on $\theta(\eta)$

Variation of We and Da:

The interaction of the Weissenberg parameter (We) with the non-Newtonian properties of tangent hyperbolic fluid is presented for scenarios both including and excluding a porous substrate. The resultant behaviour is projected in **Fig.4** and **Fig.5** affecting the velocity and temperature distribution. The behaviour of the factor We is projected for range $0 \le We \le 3$ where the factor is due to the interaction of the relaxation time factor. Here, the assigned value of We, $We = 0$ indicates the transport of Newtonian fluid, and the increasing variation led to the role of non-Newtonian tangent hyperbolic fluid on the flow profiles. The graphical illustration shows a favourable deceleration in the withy increasing Weissenberg factor i.e., the Newtonian fluid dominates over the non-Newtonian and the fluid velocity decelerates. The fact is that, Elasticity produces extra normal; stresses that decelerate the velocity gradient near the wall. Further, the behaviour is reflected in the contribution of permeability. However, the comparative result reveals that with greater porosity, the fluid velocity retards at all points as described earlier. Moreover, the greater elasticity due to the increasing We retards the fluid temperature, and the profile is asymptotic but the growing porosity augments the profile temperature greatly in comparison to non-porous medium.

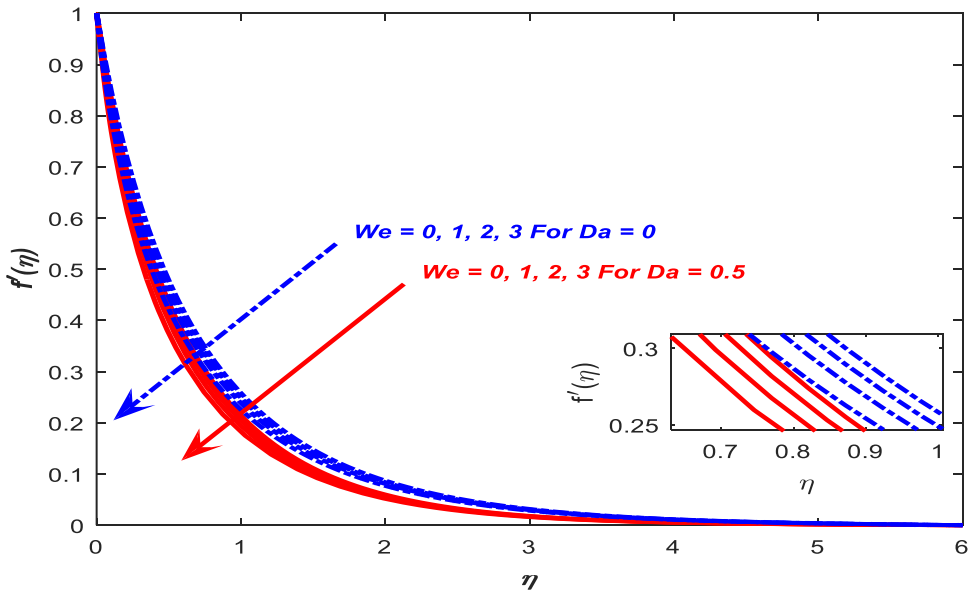

Fig.4 Various values of $f'(\eta)$ on We

ISSN No. 2454-6194 | DOI: 10.51584/IJRIAS |Volume XI Issue II February 2026

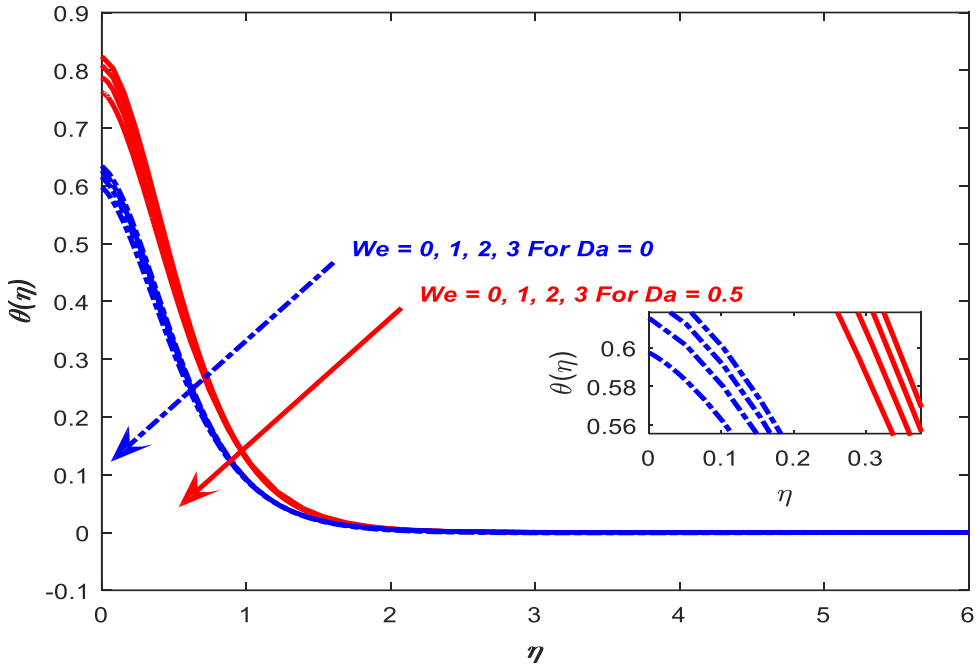

Fig.5 Various values of We on $\theta(\eta)$

Behavior of Q and Da:

The presence of the Riga plate, serving as an electromagnetic surface, emphasizes the role of the modified Hartmann number (Q) in shaping the flow profiles. **Fig.6** and **Fig.7** display the variation of the Hartmann number affecting the momentum as well as the thermal field, in which the results are depicted in several situations of $Da = 0$ and $Da = 0.5$. The modified Hartmann number is employed as a dimensionless measure to describe the impact of magnetic field strength on the motion of a conducting fluid. Observations indicate that effective magnetization imposed on the fluid over the plate substantially impacts the flow velocity. The observation reveals that for the low modified Hartmann numbers, the velocity bounding surface became thinner and it upsurges with increasing variation of the factor. It is noteworthy to execute the fact that this variation is similar to the role of permeability, and the comparative result shows that increasing permeability opposes the fluid flow due to the greater resistivity property. Further, the fluid temperature also overshoots with the increasing Hartmann number, as presented in the equivalent figure and the permeability also favours in enhancing the temperature as well.

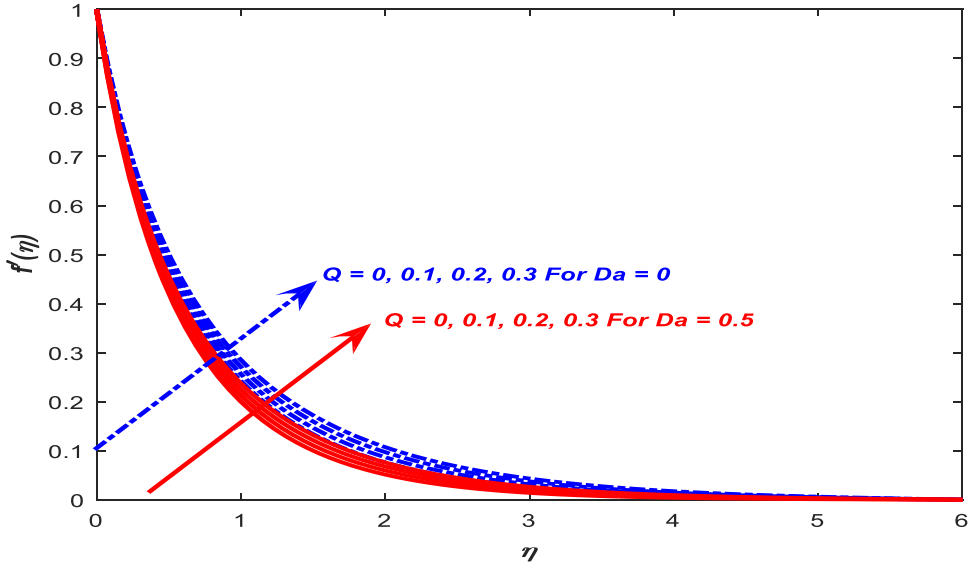

Fig.6 Various values of Q on $f'(\eta)$

ISSN No. 2454-6194 | DOI: 10.51584/IJRIAS |Volume XI Issue II February 2026

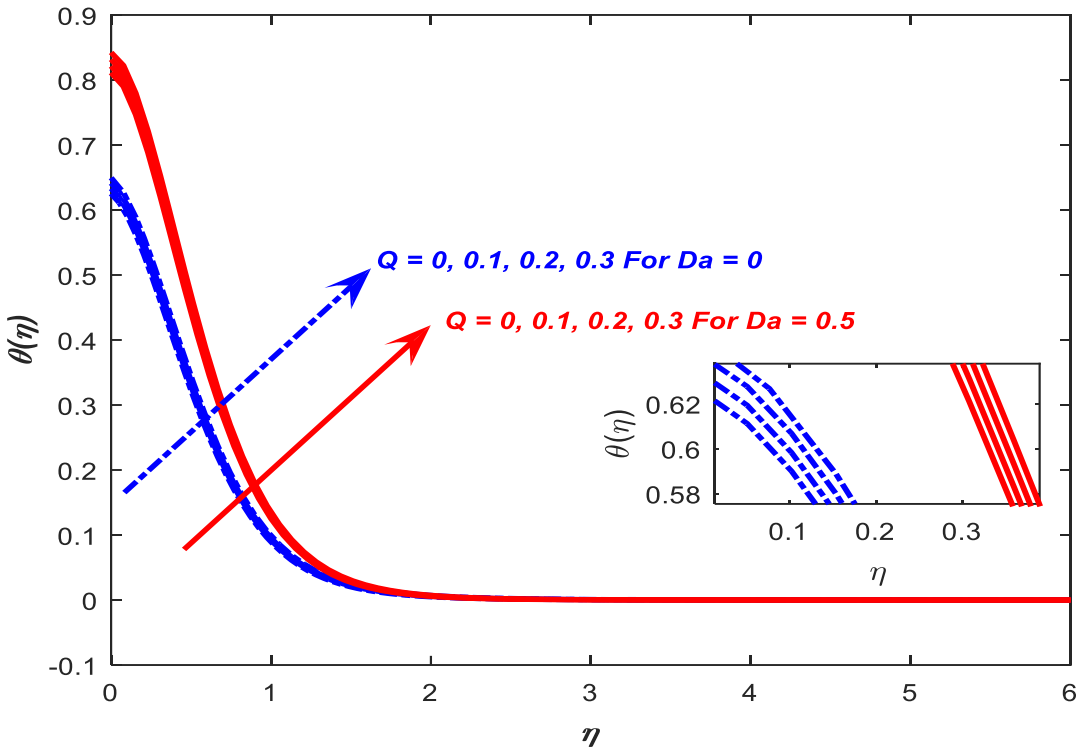

Fig.7 Various values of Q on $\theta(\eta)$

Effect of Nt, Rd, and Ec:

The cross-diffusion effect between the thermal and solutal distribution reflects the impact of thermophoresis that affects the fluid temperature. **Fig.8** reveals the significant role of thermophoresis (Nt) on the temperature distribution, considering a certain range of $0 \le Nt \le 0.6$ in a distinct case of permeability. Here, $Nt = 0$ signifies that there is no cross-diffusion among the thermal and solutal patterns. Further, the factor Nt describes due to the interaction of the temperature gradient, which leads to the transport of heat energy from the higher energy level to the lower. It is evident that higher thermophoresis causes the energy close to the surface to move upward, producing a marked rise in the energy distribution. As discussed earlier, the permeability also provides a larger influence in enhancing the thermal pattern of the non-Newtonian fluid. The insertion of nonlinear heat flux characterized by the Rosseland approximation give rise to highlights the interpretation of thermal radiation (Rd) on the fluid's energy, which is evidenced in **Fig.9**. The response is depicted for the amount of Rd within the range of $0 \le Rd \le 0.6$, where $Rd = 0$ provides the significant impact of temperature without the interaction of radiation, and the observed nonzero change demonstrates the effect of radiation on fluid temperature. The dimensionless factor appears due to the emitted electromagnetic wave from the fluid element. Further, this wave energy is transmitted to heat energy, further termed as thermal radiation. It is perceived that the enhanced values of thermal radiation display a noteworthy hike in the energy of the fluid so that the pattern elevates throughout. Moreover, this variation is projected in two distinct cases where the permeable medium encourages the temperature of the fluid at all points, which has more pronounced result than that of the flow through a transparent fluid medium. Finally, **Fig.10** describes the impact of the Eckert number (Ec) affecting the fluid temperature since the insertion of dissipative heat leads to the contribution of Ec. Here, the numerical range for the factor is considered as $0 \le Ec \le 0.6$. Physically, the factor is described as the corelation among the kinetic energy and the enthalpy difference. The increasing Ec showcases the significant deceleration in the enthalpy, which gives rise to an enhancement in the kinetic energy and consequently, the fluid temperature experiences a notable rise. This behaviour is rendered in the circumstances of a permeable/impermeable medium, and as discussed earlier, the permeable medium provides greater impact than the impermeable medium due to greater resistivity impact.

ISSN No. 2454-6194 | DOI: 10.51584/IJRIAS |Volume XI Issue II February 2026

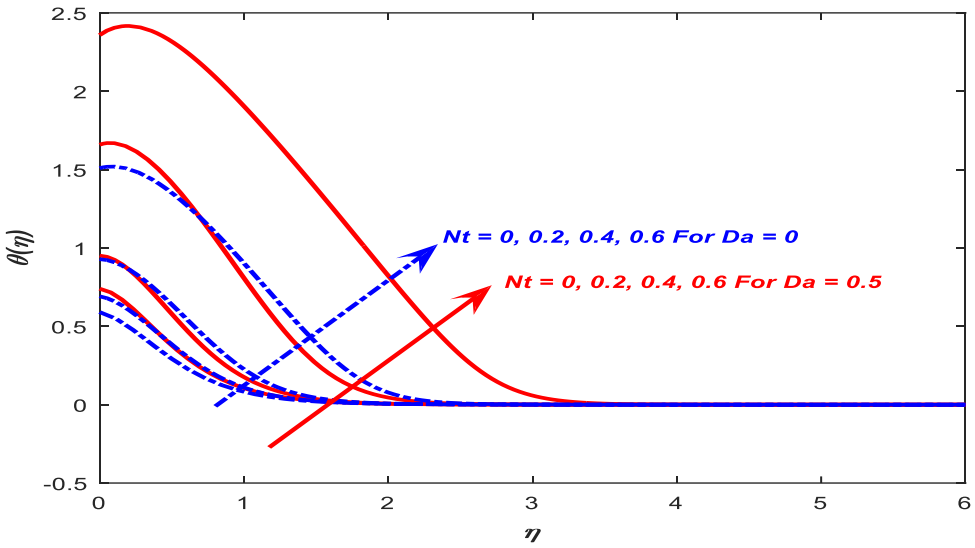

Fig.8 Various values of Nt on $\theta(\eta)$

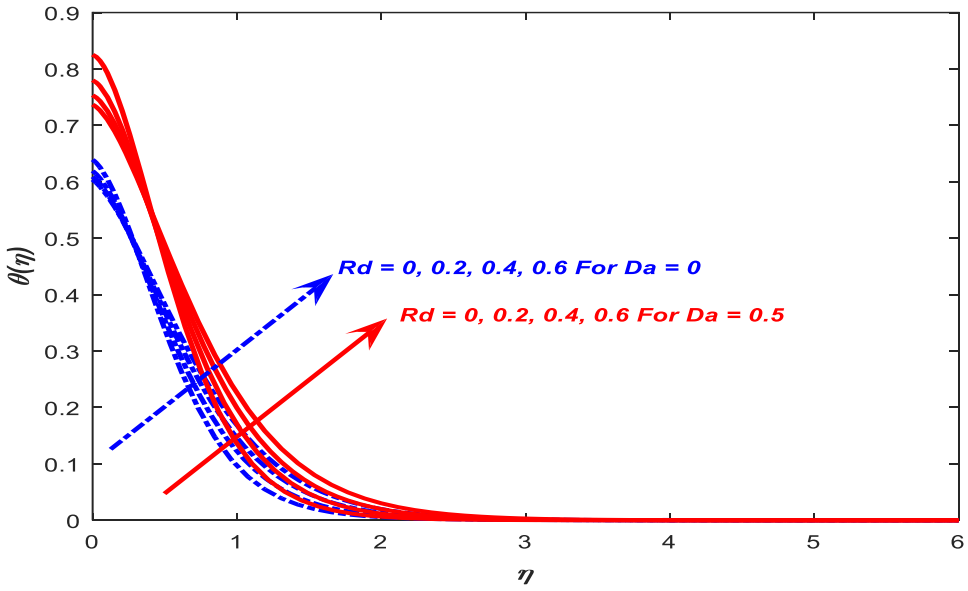

Fig.9 Various values of Rd on $\theta(\eta)$

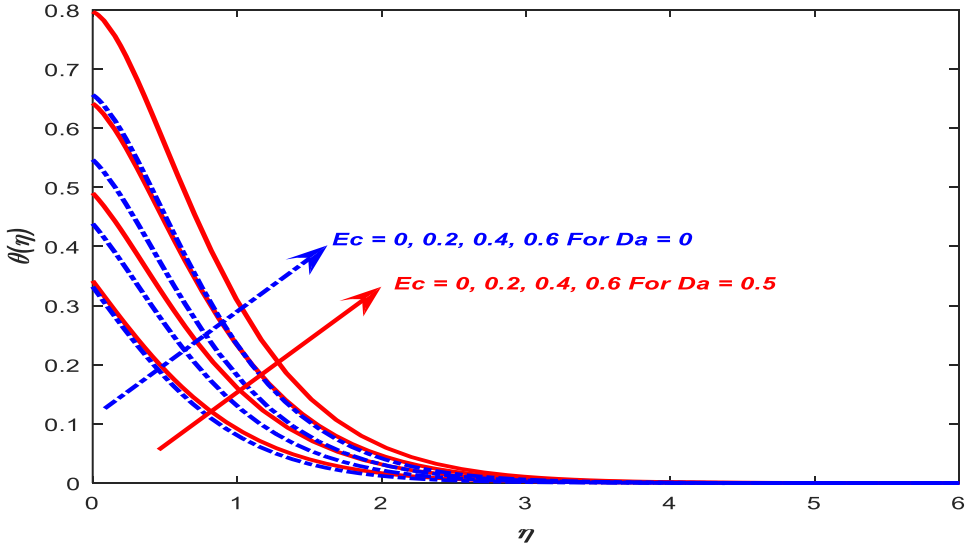

Fig.10 Various values of Ec on $\theta(\eta)$

ISSN No. 2454-6194 | DOI: 10.51584/IJRIAS |Volume XI Issue II February 2026

Significance of Le and Kc:

Several influential factors define the solutal behaviour of the nanofluid within the flow field. **Fig.11** provides the role of Lewis number (Le) on the concentration pattern, when the transportation is either via permeable/impermeable medium. The factor Le is projected for its significant variation within the range $1 \le Le \le 4$. The description of Le physically presented as the ratio of thermal diffusion and the Brownian diffusion. The lower Le signifies the dominance of the Brownian diffusion over the thermal diffusion, which shows greater concentration in magnitude within the domain. However, the higher Le shows lower Brownian diffusivity which provides a growth in the profile but the thickness of the concentration distribution. Again, the distribution of the profiles is exhibited for the distinct behaviour of permeability parameter and it reveals a greater impact for the transport through a permeable medium. The magnitude of the profile increases when the transport through permeable medium rather than the clear fluid medium. **Fig.12** portrays the behaviour of the chemical reaction term (Kc) on the concentration pattern where the variation is depicted by considering the numerical range $0 \le Kc \le 0.3$. Here, $Kc = 0$ depicts that no species is incorporated, i.e., without the role of reacting agent but the positive variation give rise to the destructive reaction on the concentration distribution. The strength of the solutal profile is maximum for the absence of reacting species whereas increasing species concentration encourages the profile as a result the thickness of the profile retards significantly. Further, the thickness of the profile becomes thinner for the absence of Da which is dominated by the flow through permeable medium.

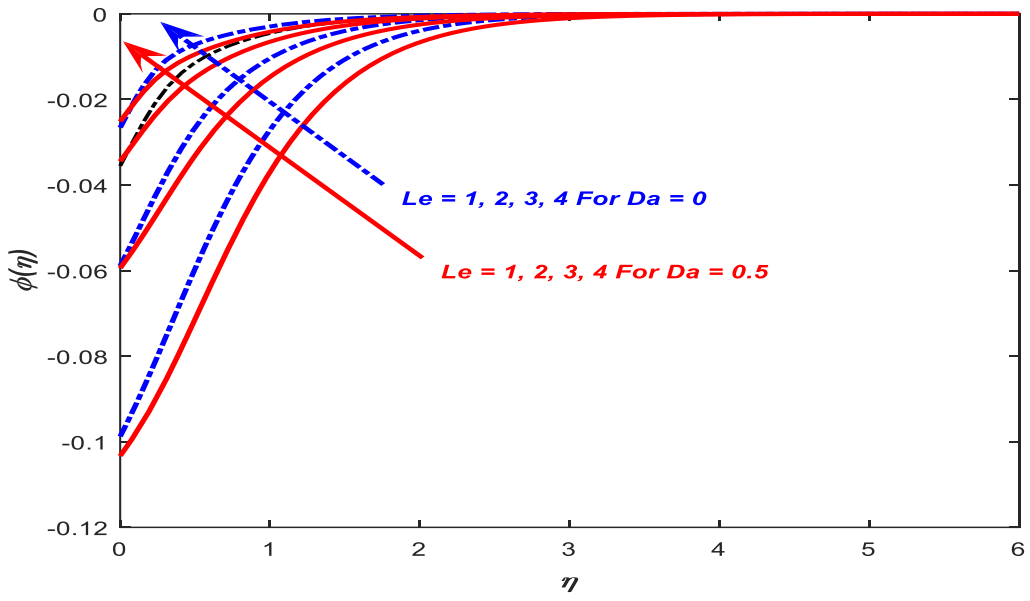

Fig.11 Various values of Le on $\phi(\eta)$

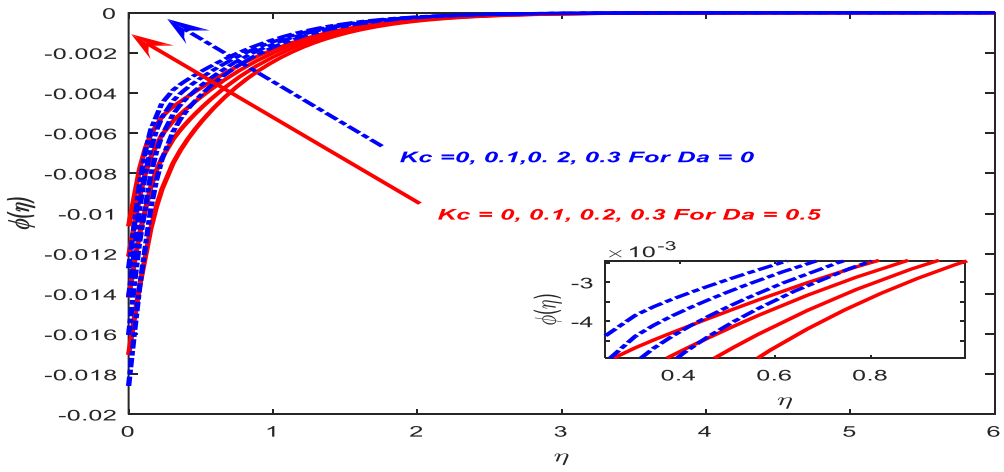

Fig.12 Various values of Kc on $\phi(\eta)$

ISSN No. 2454-6194 | DOI: 10.51584/IJRIAS |Volume XI Issue II February 2026

The bioconvection of microorganism profile is affected by several factors and these are displayed via graphs. **Fig.13** displays the characteristic of the bioconvective Lewis number (Lb) on the microorganism pattern with the variation of the factor as $1 \le Lb \le 4$. The physical description of Lb showcases a substantial corelation among the thermal diffusion and the bioconvective diffusion of the microorganism, and the higher values of Lb reveals a significant deceleration in the solutal diffusivity, which rendered attenuation in the pattern. The outline displays its greater impact For the growing diversity of the porous material that primarily influences the movement through a transparent fluid medium. Again, **Fig.14** displays the impact the Peclet number on the motile microorganism pattern which is varies within the range of $1 \le Pe \le 4$ and the results are depicted for two cases considering the impermeable medium $Da = 0$ and a permeable medium $Da = 0.5$. The enhanced Peclet number provides a thinner in the surface thickness throughout, and this behaviour is irrespective to the variation of porosity. Also, the permeability of the medium give rise to great enhancement in the profile in comparison to the flow via clear fluid medium.

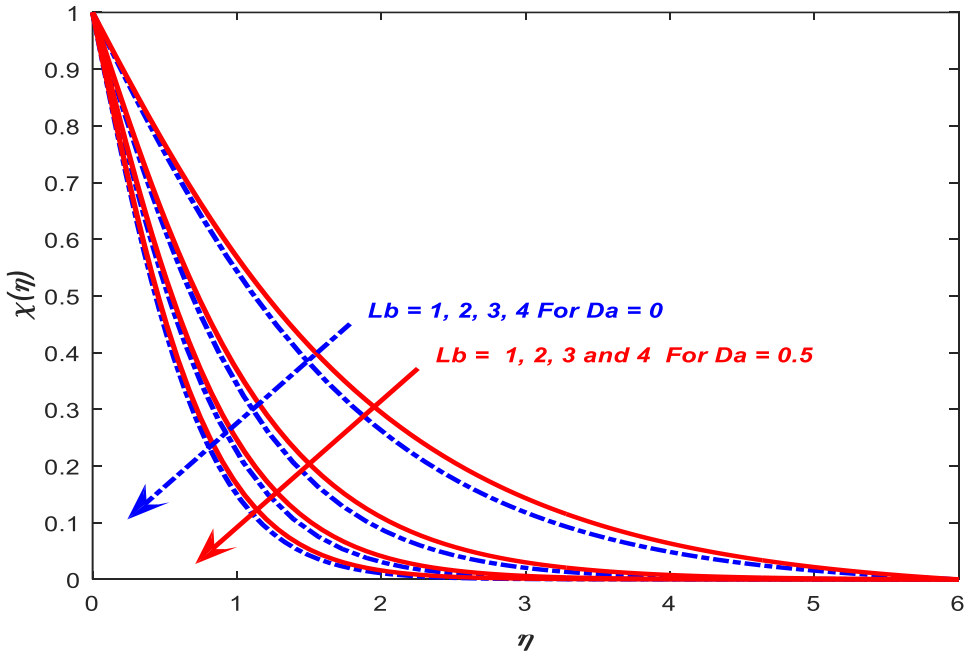

Fig.13 Various values of Lb on $\chi(\eta)$

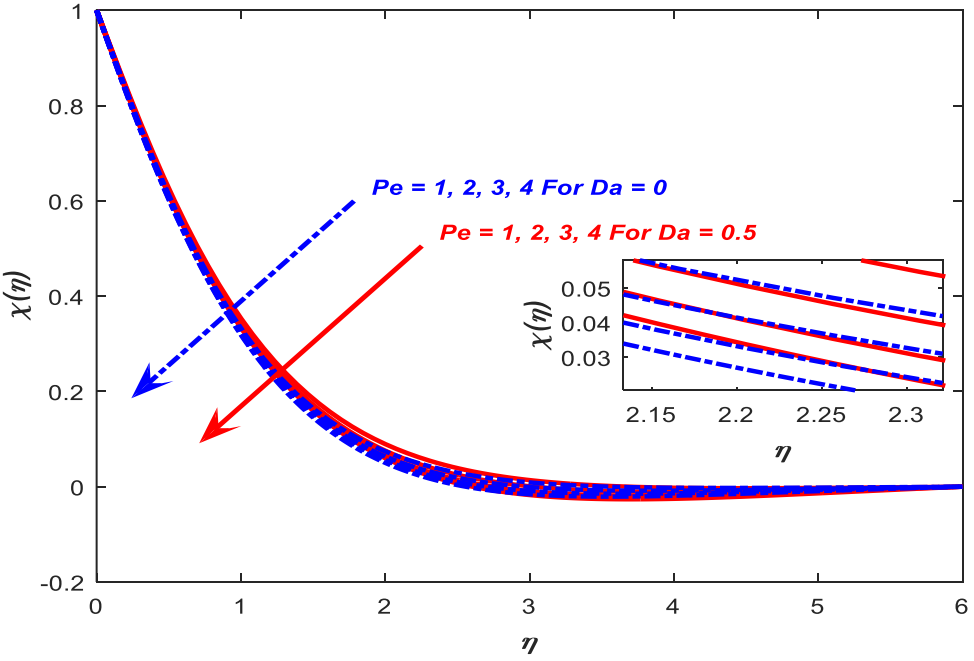

Fig.14 Various values of Pe on $\chi(\eta)$

ISSN No. 2454-6194 | DOI: 10.51584/IJRIAS |Volume XI Issue II February 2026

The evaluation of shear force, alongside the thermal conduction rate, for the fluctuation of various elements, is graphically illustrated. **Fig.15** describes the interpretation of the Weissenberg number, the non-Newtonian term on the skin friction coefficient, and the graphically depicted outcome reveals a more pronounced slowdown in the profile as the non-Newtonian characteristics intensify. This behaviour is observed for variations in porous and non-porous substrates. An enhanced permeability of the medium also favours in retarding the profile at all points and the growing region also decreases the profile irrespective of the variation of the factor. **Fig.16** illustrates the integration of magnetisation on the skin friction coefficient in two circumstances. Similar to the previous discussion, the resistance caused by magnetization combined with porosity exerts a stronger effect in slowing down the profile. The heat transfer rate caused by the interpretation of radiation is explained in **Fig.17**. It is perceived that under augmented radiant heat, the pattern of heat transfer rate amplifies considerably across the whole region, and this tendency persists regardless of whether the medium is porous or non-porous. The permeability of the medium has a dominating role over the impermeable medium, and the heat transfer rate enhances when the flow is through a permeable medium. Finally, the interpretation of Eckert number on the configuration of heat transfer rate is displayed in **Fig.18** with the variation of Da. As presented graphically, the increasing Ec, the profile enhances throughout and this variation is irrespective of the variation of Da. It is fascinating to note that close to the surface, the profile exhibits a sharper increase before gradually decelerating.

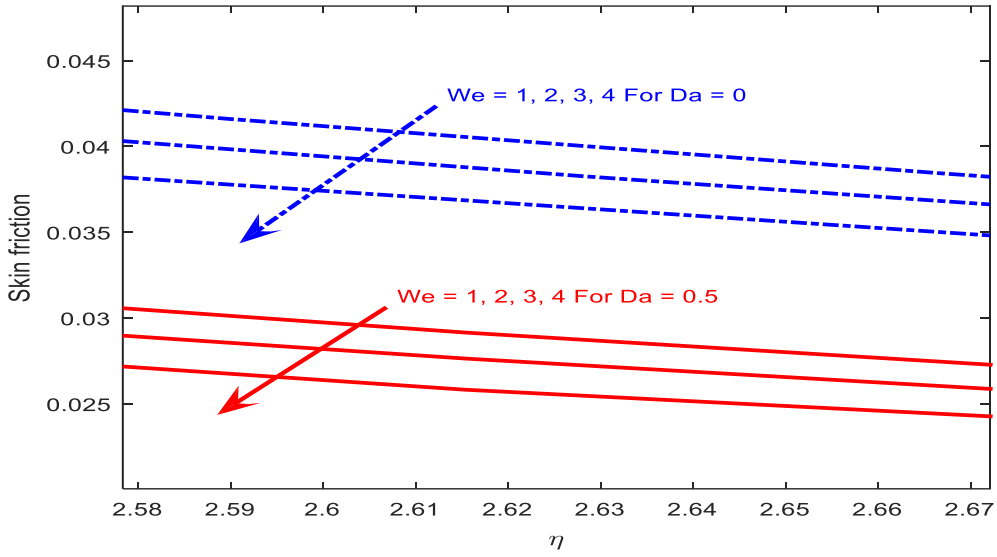

Fig.15 Various values of We on Skin friction

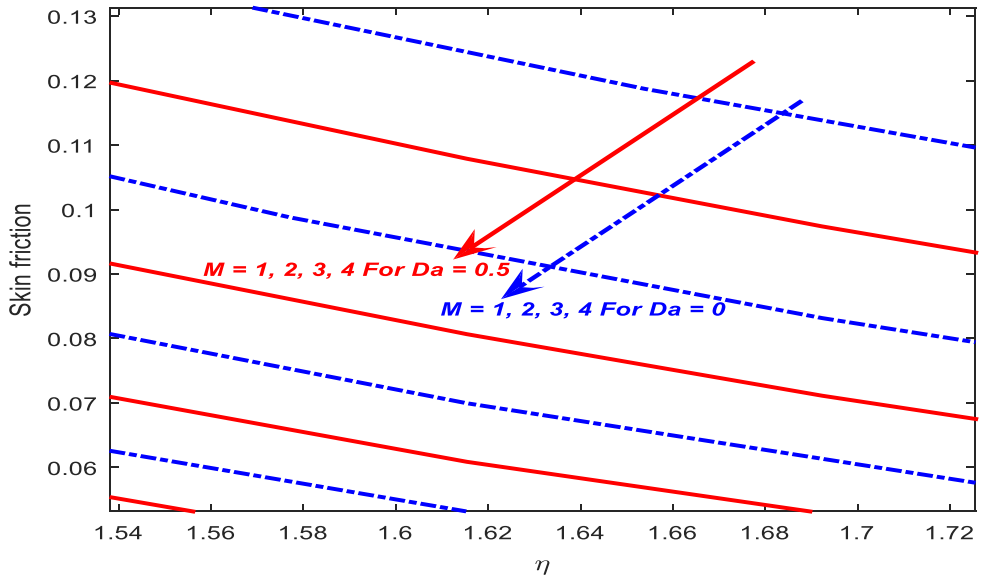

Fig.16 Various values of M on skin friction

ISSN No. 2454-6194 | DOI: 10.51584/IJRIAS |Volume XI Issue II February 2026

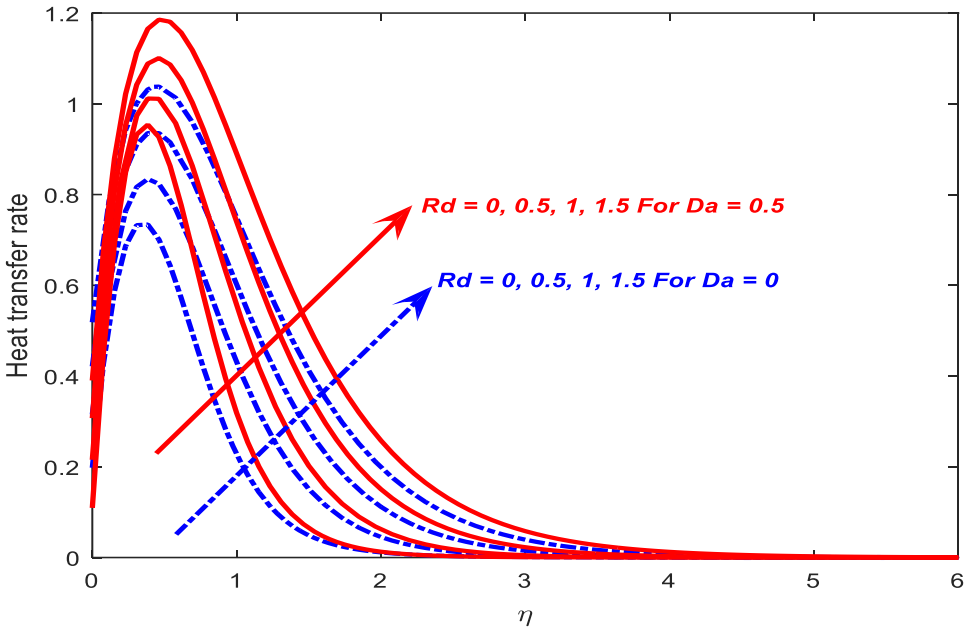

Fig.17 Various values of *Rd* on heat transfer rate

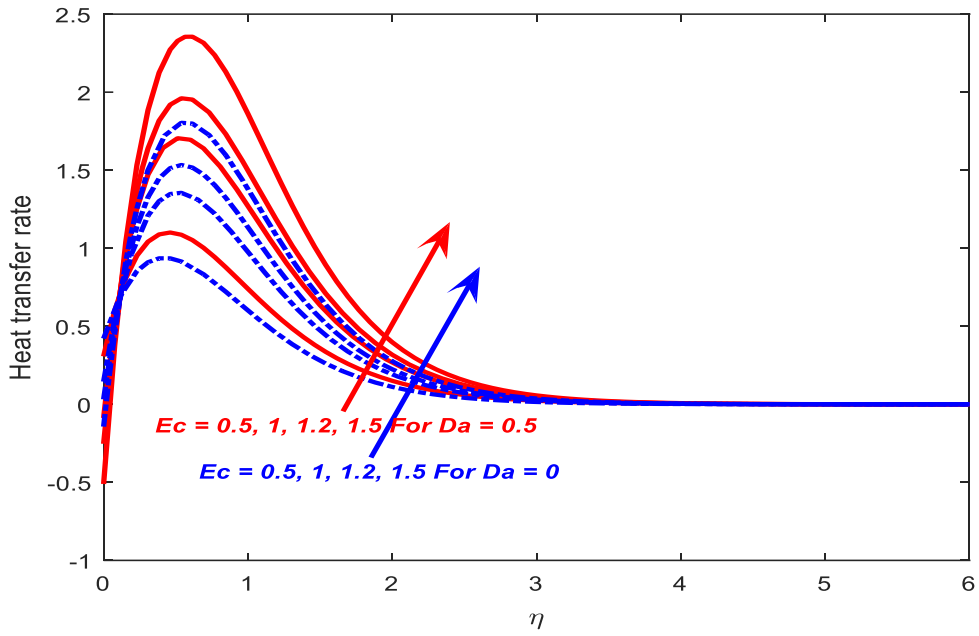

Fig.18 Various values of ***Ec*** on heat transfer rate

CONCLUSION

The present analysis conducts a numerical examination of the tangent hyperbolic nanofluid transportation of non-Newtonian nature through a Riga configuration. The impact of dissipative heat, along with the chemical reaction and thermal radiation, enriches the flow model. As a novel approach, the bioconvective induced motile microorganism encourages the two-phase flow model. The constructed mathematical model, developed by integrating the previously discussed factors, is solved computationally, with the findings represented in graphical form. The important features are reported as;

- The relative evaluation of the preceding and current study shows conformity of the solution treated as validation of the present study.
- The non-Newtonian property by the Weissenberg number is dominated by the Newtonian attributes of the fluid at all points, decelerating the thickness of the velocity bounding surface.

- The impedance arising from the application of magnetization with porosity reduces the velocity of the fluid everywhere, but conversely enhances the temperature field.

- Thermophoresis, coupled with heat radiant and the Eckert coefficient, boosts the thermal state of the non-Newtonian substance.

- Both the factors of radiating heat caused by the thermal radiation and the Eckert number caused by the dissipative heat augment the heat transfer rate.

REFERENCES

1. A.K. Abdul Hakeem, N.V. Ganesh, B. Ganga, Magnetic field effect on second order slip flow of nanofluid over a stretching/shrinking sheet with thermal radiation effect, J. Magn. Magn Mater. 381 (2015) 243–257.
2. S. Nadeem, R. Mehmood, N.S. Akbar, Combined effects of magnetic field and partial slip on obliquely striking rheological fluid over a stretching surface, J. Magn. Magn Mater. 378 (2015) 457–462.
3. N.S. Akbar, A. Ebai, Z.H. Khan, Numerical analysis of magnetic field effects on Eyring–Powell fluid flow towards a stretching sheet, J. Magn. Magn Mater. 382 (2015) 355–358.
4. F. Mabood, W.A. Khan, A.I.M. Ismail, MHD boundary layer flow and heat transfer of nanofluids over a nonlinear stretching sheet: a numerical study, J. Magn. Magn Mater. 374 (2015) 569–576.
5. I. Pop, D.B. Ingham, Convective Heat Transfer: Mathematical and Computational Modelling of Viscous Fluids and Porous Media, Elsevier, 2001.
6. M.Y. Malik, T. Salahuddin, A. Hussain, S. Bilal, MHD flow of tangent hyperbolic fluid over a stretching cylinder: using Keller box method, J. Magn. Magn Mater. 395 (2015) 271–276.
7. M. Amjad, M.N. Khan, K. Ahmed, I. Ahmed, T. Akbar, S.M. Eldin, Magnetohydrodynamics tangent hyperbolic nanofluid flow over an exponentially stretching sheet: numerical investigation, Case Stud. Therm. Eng. 45 (2023), 102900.
8. S.U. Choi, J.A. Eastman, Enhancing the Thermal Conductivity of Fluids with Nanoparticles (No. ANL/MSD/CP-84938; CONF-951135-29), Argonne National Lab., IL (United States), 1995.
9. M.D. Shamshuddin, P.S. Narayana, The combined effect of viscous dissipation and Joule heating on MHD flow past a Riga platewithCattaneo-Christovheatflux, Indian J. Phys. (2019) 1–10.
10. G. Rasool, T. Zhang, A. Shafiq, Second-grade nano-fluidic flow past a convectively heated vertical Riga plate, Phys. Scripta 94 (12) (2019), 125212.
11. R.V. Vincent, N.A. Hill, Bioconvection in a suspension of phototacticalgae, J. Fluid Mech. 327 (1996) 343–371.
12. B. Kada, I. Hussain, A.A. Pasha, W.A. Khan, M. Tabrez, K.A. Juhany, R. Othman, Significance of gyrotactic microorganism and bioconvection analysis for radiative Williamson fluid flow with ferromagnetic nanoparticles, Therm. Sci. Eng. Prog. 39 (2023), 101732.
13. Z. Raizah, A. Saeed, M. Bilal, A.M. Galal, E. Bonyah, Parametric simulation of stagnation point flow of motile microorganism hybrid nanofluid across a circular cylinder with sinusoidal radius, Open Phys. 21 (1) (2023), 20220205.
14. R. Safdar, I. Gulzar, M. Jawad, W. Jamshed, F. Shahzad, M.R. Eid, Buoyancy force and Arrhenius energy impacts on Buongiorno electromagnetic nanofluid flow containing gyrotactic microorganism, Proc. IME C J. Mech. Eng. Sci. 236 (17) (2022) 9459–9471.
15. M. Jawad, F. Mebarek-Oudina, H. Vaidya, P. Prashar, Influence of bioconvection and thermal radiation on MHD Williamson nano Casson fluid flow with the swimming of gyrotactic microorganisms due to porous stretching sheet, Journal of Nanofluids 11 (4) (2022) 500–509.
16. P.S. Reddy, P. Sreedevi, A.J. Chamkha, Heat and mass transfer flow of a nanofluid over an inclined plate under enhanced boundary conditions with magnetic field and thermal radiation, Heat Tran. Asian Res. 46 (7) (2017) 815–839.
17. P. Sreedevi, P.S. Reddy, Williamson hybrid nanofluid flow over swirling cylinder with Cattaneo–Christov heat flux and gyrotactic microorganism, Waves Random Complex Media (2021) 1–28.

18. P. Sreedevi, P.S. Reddy, Effect of SWCNTs and MWCNTs Maxwell MHD nanofluid flow between two stretchable rotating disks under convective boundary conditions, Heat Tran. Asian Res. 48 (8) (2019) 4105–4132.
19. M. Jawad, Insinuation of arrhenius energy and solar radiation on electrical conducting Williamson nano fluids flow with swimming microorganism: completion of buongiorno's model, East European Journal of Physics (1) (2023) 135–145.
20. P. Sreedevi, P.S. Reddy, A.J. Chamkha, Heat and mass transfer analysis of nanofluid over linear and non-linear stretching surfaces with thermal radiation and chemical reaction, Powder Technol. 315 (2017) 194–204.
21. P.S. Reddy, P. Sreedevi, Effect of Cattaneo–Christov heat flux on heat and mass transfer characteristics of Maxwell hybrid nanofluid flow over stretching/ shrinking sheet, Phys. Scripta 96 (12) (2021), 125237.
22. P. Sreedevi, P.S. Reddy, A.J. Chamkha, Heat and mass transfer analysis of nanofluid over linear and non-linear stretching surfaces with thermal radiation and chemical reaction, Powder Technol. 315 (2017) 194–204.
23. M. Jawad, M.K. Hameed, A. Majeed, K.S. Nisar, Arrhenius energy and heat transport activates effect on gyrotactic microorganism flowing in Maxwell bio-nanofluid with Nield boundary conditions, Case Stud. Therm. Eng. 41 (2023), 102574.
24. P. Sreedevi, P.S. Reddy, A.J. Chamkha, Magneto-hydrodynamics heat and mass transfer analysis of single and multi-wall carbon nanotubes over vertical cone with convective boundary condition, Int. J. Mech. Sci. 135 (2018) 646–655.
25. M. Jawad, M. Muti-Ur-Rehman, K.S. Nisar, Bioconvection effects on non-Newtonian chemically reacting Williamson nanofluid flow due to stretched sheet with heat and mass transfer, East European Journal of Physics (2) (2023) 359–369.
26. P. Sreedevi, P.S. Reddy, Combined influence of Brownian motion and thermophoresis on Maxwell three-dimensional nanofluid flow over stretching sheet with chemical reaction and thermal radiation, J. Porous Media 23 (4) (2020).
27. M. Jawad, K. Shehzad, R. Safdar, Novel computational study on MHD flow of nanofluid flow with gyrotactic microorganism due to porous stretching sheet, Punjab Univ. J. Math. 52 (12) (2021).
28. R. Safdar, M. Jawad, S. Hussain, M. Imran, A. Akgül, W. Jamshed, Thermal radiative mixed convection flow of MHD Maxwell nanofluid: implementation of Buongiorno's model, Chin. J. Phys. 77 (2022) 1465–1478.
29. Jawad, M., Ghazwani, H. A., Ali, M. R., Hendy, A. S., Majeed, A. H., & Wang, X. (2023). Numerical simulation for thermal radiative flow of tangent hyperbolic nanofluid due to Riga plate in the presence of joule heating. *Case Studies in Thermal Engineering*, *52*, 103686.